AJNR

Usefulness of a Rim-Enhancing Pattern on the Contrast-Enhanced 3D-FLAIR Sequence and MRI Characteristics for Distinguishing Meningioma and Malignant Dural-Based Tumor

T. Panyaping, M. Punpichet, P. Tunlayadechanont and O. Tritanon

Usefulness of a Rim-Enhancing Pattern on the Contrast-Enhanced 3D-FLAIR Sequence and MRI Characteristics for Distinguishing Meningioma and Malignant Dural-Based Tumor

T. Panyaping, M. Punpichet, P. Tunlayadechanont, and O. Tritanon

ABSTRACT

BACKGROUND AND PURPOSE: Meningiomas are the most common type of extra-axial dural-based tumors; however, malignant dural-based tumors can mimic meningiomas on imaging. The aim of this study was to determine the efficacy of differentiating meningiomas from malignant dural-based tumors by using rim-enhancement patterns on a contrast-enhanced FLAIR sequence and MR imaging characteristics.

MATERIALS AND METHODS: This retrospective study included 102 patients with meningiomas and 31 patients with malignant dural-based tumors who underwent pretreatment MR imaging. The rim-enhancement patterns on contrast-enhanced FLAIR and MR imaging characteristics, including the dural tail sign, hyperostosis, bony destruction, leptomeningeal enhancement, peritumoral edema, T2-weighted signal intensity, and tumor enhancement were evaluated.

RESULTS: Complete rim enhancement of the tumor-brain interface on contrast-enhanced FLAIR (contrast-enhanced-FLAIR rim sign) was present in most meningiomas (91/102, 89.2%) and at significantly greater frequency than in malignant dural-based tumors (2/31, 6.5%) ($P < .001$). Complete contrast-enhanced FLAIR rim enhancement provided high sensitivity (89.2%), specificity (93.5%), and accuracy (90.2%) for diagnosing meningioma. Additionally, hyperostosis was an MR imaging characteristic that suggested a diagnosis of meningioma. In contrast, bony destruction with cortical breakthrough and leptomeningeal enhancement suggested malignant dural-based tumors. There were limitations of meningiomas of <2.0 cm or at cavernous sinus locations that did not demonstrate contrast-enhanced FLAIR rim enhancement.

CONCLUSIONS: The rim-enhancement pattern on contrast-enhanced FLAIR could help differentiate meningiomas and malignant dural-based tumors. The presence of complete rim enhancement on contrast-enhanced FLAIR was a robust predictive sign for meningioma.

ABBREVIATIONS: AUC = area under the curve; CE = contrast-enhanced; NPV = negative predictive value; PPV = positive predictive value; WHO = World Health Organization

Meningioma is the most common intracranial neoplasm and extra-axial tumor, representing up to 30% of all adult intracranial neoplasms.[1] The World Health Organization (WHO) classifies meningiomas on the basis of their histologic characteristics and recurrence risk as follows: grade I, benign (80%); grade II, atypical (18%); and grade III, anaplastic/malignant (2%).

Meningiomas typically have a dual blood supply in which the primary arterial feeders from dural branches or meningeal arteries largely supply the tumor core, generating a "sunburst pattern." In large tumors, recruitment of pial supply from intracranial arteries to the peripheral parts of the tumor may be seen and provides some specific MR imaging features of rim enhancement on contrast-enhanced (CE) FLAIR images.[2,3]

In 2003, Oguz and Cila[4] investigated the enhancement patterns of meningiomas on CE-FLAIR images. Twenty-one meningiomas (70%) showed peripheral (rim) enhancement patterns, which is related to the dual (dural and pial) vascular supply to meningiomas more commonly seen in tumors of >2 cm in diameter. In 2005, Oner et al[5] found that 85% of meningiomas of >2 cm showed peripheral enhancement on the CE-FLAIR sequence, confirming the dual vascular supply. In 2014, Enokizono et al[6] revealed that

the rim-enhancement patterns on CE-FLAIR were strongly correlated with the presence of a dual vascular supply, which was evidenced by DSA, and classified the rim-enhancement patterns on CE-FLAIR into 4 grades by their extent from 0 (no rim visible) to 3 (rim visible over most of the tumor-brain interface). They also concluded that the rim-enhancement patterns on CE-FLAIR of meningioma could predict surgical cleavability and histologic tumor grade.

Meningiomas commonly present as incidental findings on brain imaging and are treated conservatively or surgically. However, approximately 2% of dural-based masses have imaging features that mimic meningiomas,[7] including primary dural neoplasms, metastases, granulomatous diseases, various inflammatory diseases, and infections.[8-11] Thus, distinguishing between meningioma and its mimics is essential because clinical management and prognosis can differ significantly, especially for malignant dural-based tumors.

In 2017, Starr and Cha[2] proposed 5 key imaging features to differentiate meningioma mimics from meningiomas, including lack of a dural tail, which was present in 83.7% of meningioma mimics, marked T2 hyperintensity (45.9%), marked T2 hypointensity (43%), osseous destruction (40.5%), and leptomeningeal extension (21.6%). In 2021, Nagai Yamaki et al[12] proposed additional dural displacement signs to predict meningioma mimics.

To the best of our knowledge, no analytic study has used rim-enhancement patterns on CE-FLAIR to differentiate meningiomas and malignant dural-based tumors. Therefore, this study aimed to distinguish these tumors on the basis of rim-enhancement patterns on CE-FLAIR and MR imaging characteristics.

MATERIALS AND METHODS
Study Setting
This retrospective study included patients treated at the Department of Diagnostic and Therapeutic Radiology of Ramathibodi Hospital between January 2015 and May 2020. The study was approved by the Institutional Ethics Committee of Ramathibodi Hospital. Because of the retrospective nature of the study, the need for informed consent was waived.

Patient Selection
This study included 133 patients with histopathologic diagnoses of meningiomas (102 patients) or malignant dural-based tumors (31 patients) who underwent pretreatment MR imaging of the brain at the Department of Diagnostic and Therapeutic Radiology of Ramathibodi Hospital between January 2015 and May 2020. All patients underwent surgical resection, and histopathologic diagnoses were made by an experienced pathologist. The 102 meningiomas (1 meningioma per person) were subdivided into 3 groups according to the WHO grading scale: WHO I, WHO II, and WHO III. Demographic data of all patients were collected from medical records.

MR Imaging Protocols and Data Acquisition
All MR imaging scans were obtained using 1.5T and 3T scanners (Ingenia; Philips Healthcare) with a standard head coil. The patients were imaged using a routine precontrast brain MR imaging protocol that included axial and sagittal T1WI, axial T2WI, axial SWI,

and DWI/ADC sequences. DWI was performed using a single-shot echo-planar imaging pulse sequence. Diffusion-sensitizing gradients were applied sequentially along the 3 orthogonal planes, and images were obtained at b-values of 0 and 1000 s/mm^2. ADC maps were generated for all patients using standard software. Routine MR imaging protocols with gadolinium (Gd) enhancement were obtained in CE-T1WI, CE-FLAIR, CE-3D T1 High Resolution Isotropic Volume Excitation (THRIVE), or BrainVIEW (Philips Healthcare). A standard dose (0.1 mmol/kg) of Gd-DTPA was injected at 1.8–2.0 mL/s in all patients using a standard length of IV tubing. After the Gd-DTPA had been injected, CE-3D FLAIR sequences were first performed in the sagittal plane with the following parameters: TR, 4800 ms; TE$_{eff}$, 330 ms; TI, 1650 ms; scan time, 5 minutes; FOV, 240 × 240 mm; matrix size, 368 × 210; and section thickness, 1.12 mm. Then, CE-3D THRIVE or BrainVIEW imaging was performed in the axial plane with TR, 5–7 ms; TE, 3–5 ms; flip angle, 12°; section thickness, 1 mm; and scan time, 2 minutes. Finally, CE T1-weighted imaging was performed with TR, 500 ms; TE, 10 ms; matrix size, 192 × 240; FOV, 240 × 240 mm; section thickness, 4 mm; and scan time, 2 minutes 15 seconds.

Imaging and Postprocessing Analysis
Axial CE-T1WI, sagittal CE-3D FLAIR, axial CE-3D THRIVE/BrainVIEW, axial T2WI, and axial DWI with ADC maps were acquired and evaluated in all patients. Multiplanar reconstruction was performed in axial, coronal, and sagittal views of the CE-FLAIR and CE-3D THRIVE/BrainVIEW images. All MR imaging findings were independently reviewed at the PACS workstation by 2 neuroradiologists with 10 and 9 years of experience in brain MR imaging. The neuroradiologists were blinded to patient data and pathologic diagnoses.

First, we evaluated the MR imaging findings including signal intensity on T2WI, dural tail (absent or present), osseous destruction (absent, marrow edema, cortex disruption, or cortical breakthrough), and hyperostosis (absent or present) on T2WI and CE-T1WI sequences. Then we defined the characteristics of rim enhancement at the tumor-brain interface as a rim with relatively high signal intensity on CE-FLAIR. We graded the rim enhancement patterns from 0 to 3 by their extent as 0, no rim visible; 1, 50% rim visible; 2, >50% rim visible but <100%; and 3, complete rim enhancement of the tumor-brain interface (100%) (Fig 1). There was no apparent discrepancy in demonstrating rim enhancement on CE-3D FLAIR images between 1.5T and 3T scanners by observation. Additionally, we evaluated leptomeningeal enhancement (absent or present) and graded peritumoral brain edema (0 to 2), which was defined as 0, no edema; 1, edema <2.0 cm radially from the tumor; and 2, edema ≥2.0 cm radially from the tumor. On CE-T1WI, we defined the contrast-enhancement pattern of the tumor as homogeneous or heterogeneous. Any discrepancies in interpretations of MR imaging findings were resolved by consensus.

Statistical Analysis
All statistical analyses were performed using STATA Version 15.1 software (StataCorp). The interobserver agreement in evaluating MR imaging characteristics was analyzed using κ analysis. A χ^2 test was used to ascertain the significance of differences in
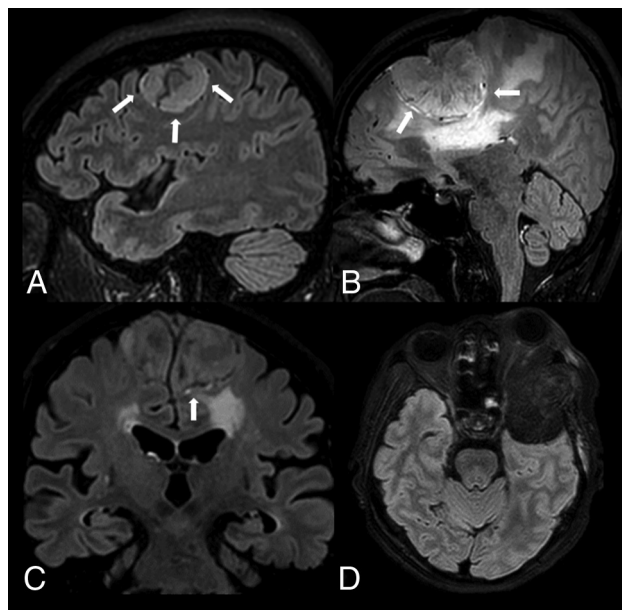
FIG 1. Four different rim-enhancement patterns at the tumor-brain interface on the CE-FLAIR sequence (*arrows*). *A*, Complete rim enhancement (CE-FLAIR rim sign). *B*, Rim enhancement of ≥50% but <100%. *C*, Rim enhancement of <50%. *D*, No visible rim enhancement. The pathologic results of *A*, *B*, and *C* are meningioma, and *D* is plasmacytoma.

Table 1: Patient demographics and pathologic findings

Variables	Meningiomas (*n* = 102, 76.7%)	Malignant Dural-Based Tumors (*n* = 31, 23.3%)
Age (mean) (yr)	51.96 (SD, 10.69)	50.03 (SD, 20.81)
Sex		
Female	85 (83.3%)	15 (48.4%)
Male	17 (16.7%)	16 (51.6%)
Size (mean) (cm)	4.37 (SD, 1.91)	4.5 (SD, 2.2)
WHO grade		
I	72 (70.6%)	–
II	22 (21.6%)	–
III	8 (7.8%)	–
Location		
Convexity	24 (23.5%)	19 (61.2%)
Sphenoid wing	20 (19.6%)	3 (9.6%)
Petroclival	18 (17.6%)	1 (3.3%)
Parafalcine	13 (12.7%)	–
Cavernous sinus	9 (8.8%)	3 (9.6%)
Cerebellopontine angle	6 (5.8%)	1 (3.3%)
Suprasellar	9 (8.8%)	–
Foramen magnum	2 (1.9%)	–
Olfactory groove	1 (0.9%)	–
Orbit	–	3 (9.6%)
Prepontine	–	1 (3.3%)

Note:—The en dash (–) indicates none.

rim-enhancement patterns on CE-FLAIR and other MR imaging characteristics between meningiomas and malignant dural-based tumors and in the subgroup analysis of meningiomas graded WHO I, WHO II, and WHO III. *P* values <.001 were considered statistically significant differences. Furthermore, we calculated the sensitivity, specificity, positive predictive value (PPV), negative predictive value (NPV), and percentage accuracy of each MR imaging characteristic for differentiating between meningiomas and

malignant dural-based tumors. Combined MR imaging features in meningiomas and malignant dural-based tumors were also analyzed to predict the diagnosis.

RESULTS

Summary of Patient Demographics and Tumor Characteristics

There were 133 patients with 133 dural-based tumors (1 mass per patient), consisting of meningiomas (102 patients, 76.7%) and malignant dural-based tumors (31 patients, 23.3%). All patient demographics and tumor characteristics are shown in Table 1. All meningiomas in this study were >2.0 cm in diameter. The 102 meningiomas were classified as WHO I (72/102, 70.6%), WHO II (22/102, 21.6%), and WHO III (8/102, 7.8%). The 31 dural-based masses were pathologically diagnosed as malignant dural-based tumors, as detailed in Table 2.

Summary of MR Imaging Findings between Meningiomas and Malignant Dural-Based Masses

Most meningiomas exhibited complete rim enhancement of the tumor-brain interface on CE-FLAIR sequences (91/102, 89.2%) (Fig 2), which was significantly higher than that in malignant dural-based tumors (2/31, 6.5%) (*P* < .001). Additionally, meningiomas frequently showed hyperostosis (76/102, 74.5%), marrow edema (76/102, 74.5%), and homogeneous enhancement on T1WI (75/102, 73.5%), features that were all significantly different compared with malignant dural-based tumors (*P* < .001), which demonstrated hyperostosis (0/31, 0%), marrow edema (6/31, 19.4%), and homogeneous enhancement on T1WI (9/31, 29%). In contrast, malignant dural-based tumors that demonstrated cortical breakthrough (21/31, 67.7%) and leptomeningeal enhancement (10/31, 32.3%), absence of a dural tail sign (6/31, 19.4%), hypointensity on T2WI (8/31, 25.8%), and heterogeneous enhancement on T1WI (22/31, 71%) were significantly different compared with meningiomas (*P* < .001), which showed cortical breakthrough (5/102, 4.9%), leptomeningeal enhancement (0/102, 0%), absence of a dural tail sign (2/102, 2%), hypointensity on T2WI (4/102, 3.9%), and heterogeneous enhancement on T1WI (27/102, 26.5%). A summary of the MR imaging findings of meningiomas and malignant dural-based tumors is presented in the Online Supplemental Data.

Characteristic MR Imaging Findings That Predict Meningiomas

Complete rim enhancement of the tumor-brain interface on the CE-FLAIR sequence demonstrated excellent sensitivity (89.2%), specificity (93.5%), PPV (97.8%), and NPV (72.5%) and had the highest accuracy (90.2%) for predicting meningioma. The interobserver agreement was excellent for interpreting rim-enhancement patterns on CE-FLAIR sequences, with a κ value = 0.902.

Furthermore, the analysis of ≥50% CE-FLAIR rim enhancement demonstrated more excellent sensitivity (95.1%), specificity (93.5%), PPV (98%), NPV (85.3%), and accuracy (94.7%) for predicting meningioma with a perfect interobserver agreement (κ value = 1.0).

Hyperostosis also showed fair sensitivity (74.5%), excellent specificity (100.0%), and PPV (100.0%) and had high accuracy

(80.5%) for consideration of meningioma. The dural tail sign and marrow edema had high sensitivity but low specificity for predicting meningioma (Table 3).

Furthermore, complete or ≥50% rim enhancement of the tumor-brain interface on the CE-FLAIR sequence (CE-FLAIR rim sign) plus hyperostosis demonstrated higher accuracy for diagnosing meningiomas of >2.0 cm (area under the curve [AUC] = 0.953).

Table 2: Characteristics of malignant dural-based tumors

Pathology	No. of Cases (n = 31)
Metastasis	18 (58%)
Adenoid cystic carcinoma	5
Lung (non-small cell)	3
Breast (invasive ductal carcinoma)	2
Squamous cell carcinoma at scalp	2
Urachal carcinoma	1
Thyroid (follicular carcinoma)	1
Mucoepidermoid carcinoma	1
Nasopharynx (SCCA)	1
Base of tongue (SCCA)	1
Colon (adenocarcinoma)	1
Plasmacytoma/multiple myeloma	6 (19.3%)
Ewing sarcoma	2 (6.4%)
Lymphoma (non-Hodgkin)	2 (6.4%)
Osteosarcoma	1 (3.4%)
Spindle cell carcinoma	1 (3.4%)
Atypical teratoid/rhabdoid tumor	1 (3.4%)

Note:—SCCA indicates squamous cell carcinoma.
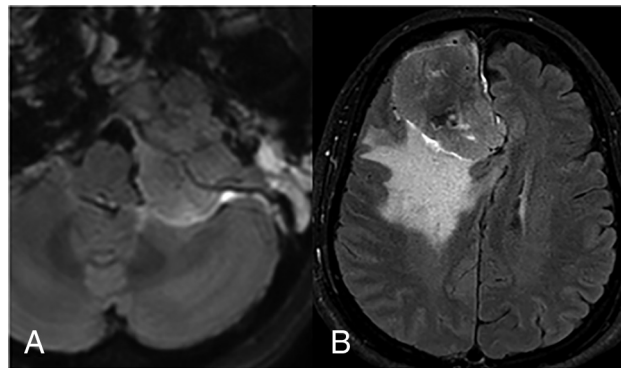
FIG 2. CE-FLAIR rim sign in meningiomas at the cerebellomedullary cistern (*A*) and parafalcine region (*B*).

Characteristic MR Imaging Findings That Predict Malignant Dural-Based Tumors

Cortical breakthrough demonstrated moderate sensitivity (67.7%) with high specificity (95.1%), PPV (80.8%), NPV (90.7%), and the best accuracy (88.7%) for consideration of malignant dural-based tumors. Leptomeningeal enhancement and lack of a dural tail demonstrated low sensitivity (32.3% and 19.4%, respectively) but high specificity (100.0% and 98.0%, respectively), PPV (100.0% and 75.0%, respectively), NPV (82.9% and 80.0%, respectively), and accuracy (84.2% and 79.7%, respectively) for predicting malignant dural-based tumors (Table 4).

A combination of aggressive MR imaging findings including leptomeningeal enhancement and cortical breakthrough was a strong predictive sign for malignant dural-based tumors (AUC = 0.911).

Subgroup Analysis of MR Imaging Findings and Comparisons between Meningiomas of WHO Grades I, II, and III

The frequency of cortical breakthrough was significantly higher in WHO grade III (4/8, 50%) meningiomas than in WHO grades I and II (1/94, 1%) ($P < .001$). WHO grade I and II meningiomas demonstrated homogeneous enhancement on T1WI (73/94, 77.6%) more often than WHO grade III meningiomas (2/8, 25%). A comparison of MR imaging findings of WHO grade I–III meningiomas is shown in the Online Supplemental Data.

DISCUSSION

Meningiomas are the most common form of intracranial neoplasms and extra-axial masses and show many specific MR imaging findings. However, approximately 2% of dural-based masses have imaging features that mimic meningiomas, specifically malignant dural-based tumors, which can be a diagnostic challenge.

During several recent years, a few studies have described rim-enhancement patterns on the CE-FLAIR sequence for diagnosing meningioma. However, no previous report in the literature has investigated the role of rim enhancement on CE-FLAIR to differentiate meningiomas and meningioma mimics. This is the first study to compare meningiomas with malignant dural-based tumors using rim-enhancement patterns on CE-FLAIR (or CE-FLAIR rim signs). In this study, the presence of a complete CE-FLAIR rim sign showed high sensitivity, specificity, PPV, and accuracy for predicting meningiomas. Most meningio-

Table 3: Characteristic MR imaging findings for predicting meningiomas

Variables	Sensitivity	Specificity	PPV	NPV	Accuracy
Dural tail sign	98.0%	19.4%	80.0%	75.0%	79.7%
Marrow edema	79.2%	33.3%	92.7%	13.0%	75.2%
Hyperostosis	74.5%	100.0%	100.0%	54.4%	80.5%
Complete rim enhancement on CE-FLAIR	89.2%	93.5%	97.8%	72.5%	90.2%
Homogeneous enhancement on T1WI	73.5%	71.0%	89.3%	44.9%	72.9%

Table 4: Characteristic MR imaging findings for predicting malignant dural-based tumors

Variables	Sensitivity	Specificity	PPV	NPV	Accuracy
Lack of dural tail	19.4%	98.0%	75.0%	80.0%	79.7%
Cortical breakthrough	67.7%	95.1%	80.8%	90.7%	88.7%
Leptomeningeal enhancement	32.3%	100.0%	100.0%	82.9%	84.2%
Heterogeneous enhancement on T1WI	71.0%	73.5%	44.9%	89.3%	72.9%
Hypointense signal on T2WI	53.3%	86.2%	66.7%	78.1%	75.0%
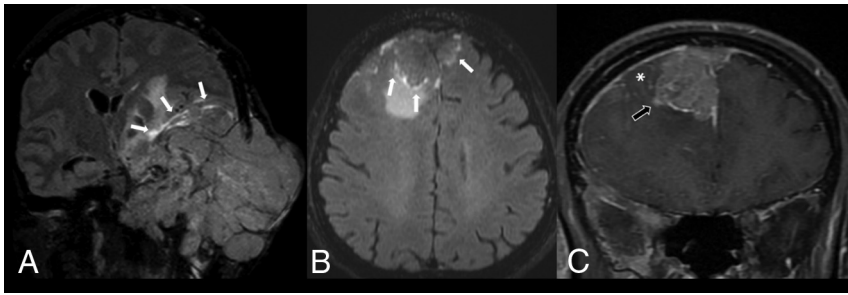
FIG 3. A, Anaplastic meningioma (WHO grade III). CE-FLAIR (A) sequence demonstrates a large extra-axial mass with cortical breakthrough involving the left middle skull base and left temporal skull with the CE-FLAIR rim sign (*white arrows*). Malignant soft-tissue tumor was the favored diagnosis in the initial report. The pathologic result is anaplastic meningioma (WHO grade III). A malignant dural-based mass on CE-FLAIR (B) and CE-T1WI fat suppression (C) sequences shows an extra-axial heterogeneously enhancing mass at the bilateral frontal convexities that had invaded the anterior-superior sagittal sinus and demonstrates the CE-FLAIR rim sign (*white arrows*), accompanied by focal leptomeningeal enhancement (*asterisk*) and adjacent brain parenchymal invasion (*black arrow*). Meningioma was the favored diagnosis in the initial report. The pathologic result was metastatic mucoepidermoid carcinoma.

mas of >2 cm demonstrated complete rim enhancement on CE-FLAIR, similar to the results presented by Oner et al[5] (12/14, 85%). Furthermore, the presence of ≥50% CE-FLAIR rim enhancement demonstrated more excellent sensitivity, specificity, and accuracy for predicting meningioma.

These characteristic MR imaging findings have been described as possibly related to the dual blood supply (meningeal and pial arterial supply) of meningiomas that is commonly seen in tumors of >2 cm in diameter (21/30, 70%).[4] Because high Gd concentrations induce signal loss in the CE-FLAIR sequence, the high concentration of Gd in the central part of meningiomas that is due to the dominant meningeal supply can suppress the T1 effect and increase T2 shortening, resulting in relative signal loss or no increased signal; in contrast, the lower concentration of Gd in the tumor capsule due to relatively less vascularity related to the pial supply can enhance T1 effects and increase T1 shortening, resulting in peripheral contrast enhancement on CE-FLAIR.[5] These findings can be observed in the CE-2D FLAIR technique in the previous studies and the CE-3D FLAIR technique in our study. In addition, the 3D-FLAIR technique has an advantage over 2D-FLAIR in multiplanar reconstruction, providing a better evaluation of the rim enhancement on CE-FLAIR.

All meningiomas in this study were >2.0 cm in diameter. Nonetheless, 4 meningiomas with no visible rim enhancement and 1 meningioma with <50% rim enhancement on CE-FLAIR were observed. All 4 meningiomas with nonvisible rim enhancement were located in the intracavernous sinuses and received vascular supply in various ways from the ICA (C3–C7 segments), ophthalmic artery, or intracranial branches of the external carotid artery without pial vascular supply except for those that extended beyond the cavernous sinus.[13] Such findings represented a limitation of using CE-FLAIR rim signs to predict intracavernous meningiomas (Online Supplemental Data). The meningioma that demonstrated <50% CE-FLAIR rim enhancement was located at the cerebral convexity. The reduced rim enhancement of this lesion could be related to the relatively poor pial artery supply of the tumor.

Recent studies suggest that malignant dural-based masses receive vascular supply from various branches of the internal and external carotid arteries according to their cell types and locations.[14-16] No pial vascular supply in the tumor capsule has been described for malignant dural-based masses. However, our study demonstrated 2 cases of malignant dural-based tumors (dural metastasis of squamous cell carcinoma and mucoepidermoid carcinoma) with complete rim enhancement on the CE-FLAIR sequence accompanied by aggressive imaging features, including adjacent leptomeningeal enhancement and brain parenchymal invasion. The CE-FLAIR rim sign of these lesions could be related to prominent pial arterial supply at the peripheral portion of the tumors (Fig 3).

In this study, bony hyperostosis demonstrated fair sensitivity and excellent specificity and PPV, with high accuracy for consideration of meningioma, consistent with findings in prior literature.[17] However, lymphomas and immunoglobulin G4–related diseases can show hyperostosis that can mimic meningioma,[18,19] but we did not observe this feature in this study.

A dural tail was a hallmark for meningioma, with almost 60% prevalence, but several dural-based masses also demonstrated this feature.[20,21] The proliferation of meningiomas triggers an inflammatory reaction that results in dural thickening and enhancement. In this study, a dural tail was present in 98% of meningiomas and 80.6% of malignant dural-based tumors ($P < .001$), higher than what was previously reported for the prevalence of dural tails in meningioma mimics by Starr and Cha.[2] Furthermore, in our study, the lack of a dural tail demonstrated relatively low sensitivity but high specificity for predicting malignant dural-based tumors compared with the study by Starr and Cha.

The presence of cortical breakthrough in dural-based masses represents an aggressive feature with significant bone destruction, which is supposed to be found in malignant dural-based tumors and WHO grade III meningiomas and is very unusual in WHO grade I meningiomas.[2] Our study found that cortical breakthrough had moderate sensitivity, high specificity, good PPV and NPV, and the highest accuracy for consideration of malignant dural-based tumors, similar to the results of Starr and Cha.[2] However, there were 5 cases of meningiomas that demonstrated cortical breakthrough. All were anaplastic meningiomas (WHO III) with complete rim enhancement on CE-FLAIR sequences, features that could help suggest anaplastic or malignant meningioma rather than malignant dural-based tumors (Fig 3).

Additionally, leptomeningeal enhancement was an excellent predictive sign for malignant dural-based tumors and was not generally seen in meningiomas. Our study demonstrated adjacent leptomeningeal enhancement in metastases, lymphoma, atypical teratoid/rhabdoid tumor, and squamous cell carcinoma at the scalp, possibly related to the subarachnoid space and brain parenchymal invasion. Therefore, observing associated leptomeningeal
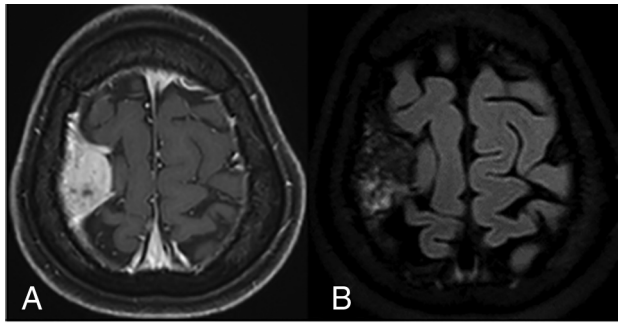
FIG 4. *A,* CE-T1WI fat suppression sequence demonstrates an extra-axial mass at the right frontoparietal convexity with a dural tail sign that resembles a meningioma. *B,* CE-FLAIR sequence. No rim enhancement on the tumor-brain interface is observed. Meningioma was the favored diagnosis in the initial report. The pathologic result was osteosarcoma.

enhancement could alert radiologists that a dural-based mass is unlikely to be a meningioma.[2]

Hypointensity on T2WI is a feature that is not commonly seen in meningiomas and generally indicates hypercellularity, large areas of calcification, or significant fibrous tissue in the tumor, which are variably present in meningioma mimics. In this study, 25.8% (8/31) of malignant dural-based tumors showed hypointensity on T2WI. They were metastases, plasmacytoma/multiple myeloma, and osteosarcoma (Fig 4). The frequency of hypointensity on T2WI was lower compared with the findings of Starr and Cha,[2] in which 43% of malignant dural-based tumors had hypointensity on T2WI. Homogeneous or heterogeneous enhancement on T1WI was variable in each tumor type and histologic subtype of meningioma.[22]

Thus, combining these MR imaging findings could lead to high accuracy in differentiating meningioma and malignant dural-based tumors. Complete or ≥50% rim enhancement of the tumor-brain interface on the CE-FLAIR sequence (the CE-FLAIR rim sign) plus hyperostosis demonstrated higher accuracy for diagnosing meningiomas of >2.0 cm (AUC = 0.953), except for those at an intracavernous location. However, CE-FLAIR rim signs were found in a few malignant dural-based masses, where they were accompanied by leptomeningeal enhancement and brain parenchymal invasion. Therefore, aggressive MR imaging findings including leptomeningeal enhancement and cortical breakthrough were strong predictive signs of malignant dural-based tumors (AUC = 0.911). In this study, cortical breakthrough was present in 4 cases of WHO grade III meningiomas. However, these cases also had complete CE-FLAIR rim signs, findings that were highly suggestive of meningioma with aggressive behavior. Regarding the results from our study, we have proposed the diagnostic framework for differentiating meningioma and malignant dural-based tumor, which is shown in the Online Supplemental Data.

Our study had some limitations, including its single-institution nature, no evaluation of tumors of <2.0 cm in diameter, and a small number of WHO grade III meningiomas. Further studies should include more patients, specifically with WHO grade III meningioma. Nevertheless, this study is the first step toward using rim-enhancement patterns on CE-FLAIR to predict meningioma

and differentiate such cases from malignant dural-based tumors. Future research could use rim-enhancement patterns on CE-FLAIR and other MR imaging findings to differentiate meningiomas and other benign dural-based masses such as hemangiopericytomas and infectious/inflammatory dural-based lesions, which can mimic each other and make diagnostics challenging.

CONCLUSIONS

Complete or ≥50% rim enhancement on the CE-FLAIR sequence (CE-FLAIR rim sign) showed high accuracy for diagnosing meningiomas of >2.0 cm. Hyperostosis was another helpful MR imaging finding for predicting meningioma. Aggressive MR imaging findings including cortical breakthrough and leptomeningeal enhancement were strong predictive signs of malignant dural-based tumors.

Disclosure forms provided by the authors are available with the full text and PDF of this article at www.ajnr.org.

REFERENCES

1. Osborn AG. *Brain Imaging, Pathology, and Anatomy.* 2nd ed. Elsevier; 2017:659–94
2. Starr CJ, Cha S. **Meningioma mimics: five key imaging features to differentiate them from meningiomas.** *Clin Radiol* 2017;72:722–28 CrossRef Medline
3. Kelly M. Tumors. In: Krings T, Geibprasert S, ter Brugge KG eds. *Case-Based Interventional Neuroradiology.* Thieme Medical Publishers; 2011:207–12
4. Oguz KK, Cila A. **Rim enhancement of meningiomas on fast FLAIR imaging.** *Neuroradiology* 2003;45:78–81 CrossRef Medline
5. Oner AY, Tokgöz N, Tali ET, et al. **Imaging meningiomas: is there a need for post-contrast FLAIR?** *Clin Radiol* 2005;60:1300–05 CrossRef Medline
6. Enokizono M, Morikawa M, Matsuo T, et al. **The rim pattern of meningioma on 3D FLAIR imaging: correlation with tumor-brain adhesion and histological grading.** *Magn Reson Med Sci* 2014;13:251–60 CrossRef Medline
7. Ghosal N, Dadlani R, Gupta K, et al. **A clinicopathological study of diagnostically challenging meningioma mimics.** *J Neurooncol* 2012;106:339–52 CrossRef Medline
8. Smith AB, Horkanyne-Szakaly I, Schroeder JW, et al. **From the radiologic pathology archives: mass lesions of the dura: beyond meningioma-radiologic-pathologic correlation.** *Radiographics* 2014;34:295–312 CrossRef Medline
9. Nayak L, Abrey LE, Iwamoto FM. **Intracranial dural metastases.** *Cancer* 2009;115:1947–53 CrossRef Medline
10. Lee EK, Lee EJ, Kim MS, et al. **Intracranial metastases: spectrum of MR imaging findings.** *Acta Radiol* 2012;53:1173–85 CrossRef Medline
11. Meyers SP, Hirsch WL Jr, Curtin HD, et al. **Chondrosarcomas of the skull base: MR imaging features.** *Radiology* 1992;184:103–08 CrossRef Medline
12. Nagai Yamaki V, de Souza Godoy LF, Alencar Bandeira G, et al. **Dural-based lesions: is it a meningioma?** *Neuroradiology* 2021;63:1215–25 CrossRef Medline
13. Schramm J. *Advances and Technical Standards in Neurosurgery.* Vol 43. Springer-Verlag; 2015:103–22
14. Lyndon D, Lansley JA, Evanson J, et al. **Dural masses: meningiomas and their mimics.** *Insights Imaging* 2019;10:11 CrossRef Medline
15. Hayt DB, Blatt CJ, Goldman SM, et al. **Hypervascular presentation of multiple myeloma involving the skull, demonstrated on encephaloscintigraphy.** *J Nucl Med* 1979;20:125–26 Medline
16. Whitehead RE, Melhem ER, Kasznica J, et al. **Telangiectatic osteosarcoma of the skull base.** *AJNR Am J Neuroradiol* 1998;19:754–57 Medline

17. Siegelman ES, Mishkin MM, Taveras JM. **Past, present, and future of radiology of meningioma.** *Radiographics* 1991;11:899–910 CrossRef Medline

18. Paiva J, King J, Chandra R. **Extra-axial Hodgkin's lymphoma with bony hyperostosis mimicking meningioma.** *J Clin Neurosci* 2011;18:725–27 CrossRef Medline

19. Lin CK, Lai DM. **IgG4-related intracranial hypertrophic pachymeningitis with skull hyperostosis: a case report.** *BMC Surg* 2013;13:37 CrossRef Medline

20. Wilms G, Lammens M, Marchal G, et al. **Thickening of dura surrounding meningiomas: MR features.** *J Comput Assist Tomogr* 1989;13:763–68 CrossRef Medline

21. Wilms G, Lammens M, Marchal G, et al. **Prominent dural enhancement adjacent to nonmeningiomatous malignant lesions on contrast-enhanced MR images.** *AJNR Am J Neuroradiol* 1991;12:761–64 Medline

22. Kunimatsu A, Kunimatsu N, Kamiya K, et al. **Variants of meningiomas: a review of imaging findings and clinical features.** *Jpn J Radiol* 2016;34:459–69 CrossRef Medline